Nutrient supplementation experiments with saltern microbial communities implicate utilization of DNA as a source of phosphorus

Running Title: DNA as a microbial community's phosphorus source

Zhengshuang Hua[1], Matthew Ouellette[2,$], Andrea M. Makkay[2], R. Thane Papke[2,*], Olga Zhaxybayeva[1,3*]

[1] Department of Biological Sciences, Dartmouth College, Hanover, NH, USA

[2] Department of Molecular and Cell Biology, University of Connecticut, Storrs, CT, USA

[3] Department of Computer Science, Dartmouth College, Hanover, NH, USA

[$] Current affiliation: The Forsyth Institute, Cambridge, Massachusetts, USA and Department of Oral Medicine, Infection and Immunity, Harvard School of Dental Medicine, Boston, Massachusetts, USA

[*]Corresponding authors:

O.Z., olga.zhaxybayeva@dartmouth.edu;

R.T.P., thane@uconn.edu.

Keywords: extracellular DNA, dissolved DNA, hypersaline, haloarchaea, Halobacteria, DNA uptake, community diversity

Abstract

All environments including hypersaline ones harbor measurable concentrations of dissolved extracellular DNA (eDNA) that can be utilized by microbes as a nutrient. However, it remains poorly understood which eDNA components are used, and who in a community utilizes it. For this study, we incubated a saltern microbial community with combinations of carbon, nitrogen, phosphorus, and DNA, and tracked the community response in each microcosm treatment via 16S rRNA and *rpoB* gene sequencing. We show that microbial communities used DNA only as a phosphorus source, and provision of other sources of carbon and nitrogen was needed to exhibit a substantial growth. The taxonomic composition of eDNA in the water column changed with the availability of inorganic phosphorus or supplied DNA, hinting at preferential uptake of eDNA from specific organismal sources. Especially favored for growth was eDNA from the most abundant taxa, suggesting some haloarchaea prefer eDNA from closely related taxa. Additionally, microcosms' composition shifted substantially depending on the provided nutrient combinations. These shifts allowed us to predict supplemented nutrients from microbial composition with high accuracy, suggesting that nutrient availability in an environment could be assessed from a taxonomic survey of its microbial community.

Introduction

Dissolved extracellular DNA (eDNA) in the environment plays important roles in global cycles of carbon (C), nitrogen (N) and phosphorus (P). It is found at measurable concentrations in every analyzed habitat [1–4] and is estimated to amount to gigatons globally [5]. Presence of eDNA in environments is predominantly influenced by release of DNA via microbial cell lysis from viral infections [6, 7], but also results from DNA freed up from spontaneous and programmed cell death, autolysis, and direct DNA secretion [8–11]. Subsequently, eDNA becomes available for resident organisms to utilize, and in some environments eDNA turnover rates can be as short as a few hours [12]. However, seasonal variability and type of habitat can increase the residence time of eDNA to months and years [13, 14], despite the presence and high activity of secreted extracellular nucleases [3]. Adsorption to minerals and particles can make eDNA unavailable for microorganisms [15], but factors like nutrient obtainability, and the presence of salt could also contribute to the stability, availability and utilization of the available eDNA [13, 16].

Many microorganisms secrete enzymes that degrade eDNA extracellularly [17]. The subsequent uptake of the DNA components could be used to support growth by being used as a C, N or P source [18, 19]. Many archaea and bacteria can also take up double-stranded eDNA as a high molecular weight molecule via a process of natural transformation, and use it either to repair damaged chromosomes or to increase genetic variation [15, 20]. However, since natural transformation has low efficiency rates and only one DNA strand is typically used in recombination, most of the eDNA transported into the cell may be consumed for other purposes, such as an energy source or as input building blocks (e.g., nucleotides) in metabolic pathways [21–25].

57 Hypersaline environments are reported to have the highest concentrations of eDNA [3]. These
58 habitats have little to no primary production near the saturation level of NaCl, yet they support a high
59 density of cells, usually dominated by heterotrophic, aerobic, obligate halophilic archaea, informally
60 known as Haloarchaea [26–28]. A nutritionally competent model haloarchaeon *Haloferax volcanii* can
61 grow on eDNA, primarily as a P source [29], suggesting that in hypersaline habitats eDNA plays an
62 important role in the phosphorus cycle and also possibly in carbon and nitrogen cycles. Notably, *Hfx.*
63 *volcanii* discriminates different eDNA sources for growth, as cultures did not grow on purified *E. coli* or
64 herring sperm DNA, but grew on *Hfx. volcanii* (i.e., its own) or unmethylated *E. coli* DNA [23]. Although
65 some bacteria have demonstrated biased uptake of DNA for natural transformation purposes [30–33], the
66 above observations for *Hfx. volcanii* raise the possibility that many other microorganisms in a
67 haloarchaeal community can grow only on specific eDNA, perhaps based on its methylation status. This
68 remains a largely unexplored phenomenon. To better understand how eDNA influences growth of
69 microbial communities in hypersaline environments, and to investigate eDNA utilization biases associated
70 with organismal source of eDNA by different haloarchaea and hypersaline-adapted bacteria, we
71 conducted microcosm experiments on natural near-saturated hypersaline waters collected from the Isla
72 Cristina solar saltern in southern Spain that were amended by sources of C, N, inorganic phosphorus (P_i)
73 and DNA. We show that eDNA, which was either available in the water column or provided as a
74 supplement, was utilized by the microbial community as a source of phosphorus. Via sequencing of *rpoB*
75 and 16S rRNA genes from DNA collected from both the cells and water column before and after the
76 experiments, we observe that composition of both microbes in the community and eDNA in the water

77 column changes depending on nutrients, and infer that at least some of these shifts are due to the ability to
78 use eDNA and to prefer eDNA of specific taxonomic origin or taxonomic relatedness. We also found that
79 the shifts in taxonomic composition of a saltern microbial community and eDNA in the water column are
80 substantial enough to be predictive of the provided nutrients.
81

82 **Materials and Methods**

83 *Nutrient supplementation of samples, microcosms' incubation, DNA purification,* rpoB *and 16S rRNA*
84 *genes amplification*

85 Isla Cristina water samples were aliquoted into 50mL conical tubes, with each tube receiving 30mL of
86 water sample. These samples were supplemented with various combinations of C (0.5% w/v glucose), N
87 (5 mM NH_4Cl), and P_i (1 mM KH_2PO_4) sources, as well as with high molecular weight, undigested
88 genomic DNA (~6ng/µL of either *Hfx. volcanii* DS2 or *E. coli dam*$^-$/*dcm*$^-$) (the listed concentration values
89 are final concentrations). Each combination of nutrient supplementation was performed in duplicate. The
90 microcosms were incubated at 42°C and once they reached stationary phase, they were centrifuged and
91 filtered. DNA was extracted, and *rpoB* and 16S rRNA genes were PCR-amplified. For details see
92 **Supplementary Methods.**
93

94 *Quantification of nutrients in Isla Cristina water samples*

95 The Isla Cristina water samples before and after experiments (including duplicates) were analyzed for
96 total organic carbon (TOC), total dissolved nitrogen (TN), total phosphorus (TP) and inorganic
97 phosphorus (P_i). For each microcosm, 5 mL was aliquoted into 50 mL conical tubes, which were then

98 diluted 1:10 with deionized water. The organic phosphorus in each sample (P_o) was calculated as the
99 difference between TP and P_i. See **Supplementary Methods** for details.
100
101 *DNA sequencing, sequence quality control, pair merging, clustering of sequences into the operational*
102 *taxonomic units and assignment of taxonomic affiliations*
103 The purified amplicon products were used to construct 69 *rpoB*-based and 28 16S-rRNA-based libraries.
104 The libraries were sequenced using Illumina MiSeq technology, collectively producing 3 567 797 and 2
105 277 899 paired-end raw reads for *rpoB* and 16S-rRNA genes, respectively. The raw reads were trimmed
106 from poor quality regions and pairs were merged as described in **Supplementary Methods**. This
107 procedure resulted in the 1 174 289 *rpoB* and 1 320 673 16S *rRNA* merged pairs, which were clustered
108 into operational taxonomic units (OTUs) using QIIME v1.9.1 [34] and assigned taxonomic affiliations
109 using the Ribosomal Database Project classifier v2.2 [35], as detailed in **Supplementary Methods**. Since
110 *E. coli* and *Hfx. volcanii* are not indigenous members of the initial microbial community, the DNA
111 assigned to these taxa were excluded from all further analyses.
112
113 *Quantification of similarities and differences in taxonomic composition across and within samples*
114 For each sample, relative abundance of its OTUs, overall taxonomic composition and the OTU diversity
115 were calculated as described in **Supplementary Methods**. Additionally, the samples were clustered via
116 Principal Coordinates Analysis (PCoA), using beta-diversity distances calculated from Bray-Curtis and
117 Jaccard dissimilarity values. The clusters were tested for similarity and differences in the OTU

118 composition (see **Supplementary Methods** for details).

119

120 *Examination of the impact of provided nutrients on community composition using linear regression*

121 Linear regression modeling was conducted with provided nutrients (C, N, P_i and P_o) as explanatory

122 variables and number of OTUs in each sample as dependent variables as described in **Supplementary**

123 **Methods**.

124

125 *Quantification of changes in relative abundances of the abundant haloarchaeal OTUs (ahOTUs) in*

126 *response to provided phosphorus*

127 Changes in ahOTU abundance in microcosms and eDNA pools in response to addition of DNA and P_i

128 were visualized as heatmaps mapped to a cladogram of relationships among ahOTUs (see

129 **Supplementary Methods** for details). Additionally, changes in relative abundance of an ahOTU in

130 microcosms and eDNA pools between two experimental treatments were summarized using two metrics,

131 $D = (ICW_a - ICW_b) - (ICC_a - ICC_b)$ and $ln(Odds\ ratio) = \ln(\frac{ICW_a/ICW_b}{ICC_a/ICC_b})$, where a and b denote two

132 compared treatments and ICC_i and ICW_i represent relative abundances of an ahOTU in communities and

133 eDNA pools of a treatment i, respectively.

134

135 *Prediction of provided nutrients from taxonomic composition of a sample*

136 Using the relative abundance of ahOTUs in a sample and categorization based on combination of

137 nutrients provided in the experiments, a random forest classifier [36] was trained and cross validated as

138 described in **Supplementary Methods**. The performance of classifier trained on the real data was

139 compared to that of a classifier trained on the re-shuffled samples.

140

141 *Data availability*

142 Raw sequencing data is available in GenBank under BioProject ID PRJNA646965. **Supplementary**

143 **Data**, which includes a script used for raw data quality control, merged pairs, database used for *rpoB*-

144 based OTU taxonomy assignment, tables of OTU composition per sample, and nucleotide sequences

145 chosen to represent each OTU, are available in FigShare repository at

146 https://doi.org/10.6084/m9.figshare.12609068.

147

148 **Results**

149 **Isla Cristina's microbial communities grow on eDNA as a phosphorus source**

150 Supplementation of microbial communities from the Isla Cristina saltern (Huelva, Spain) with various

151 combinations of C, N, P_i, and DNA from either *Hfx. volcanii* DS2 (denoted as H) or *E. coli dam*$^-$/*dcm*$^-$

152 (denoted as E) revealed that unless both C and N were provided, no notable growth was observed (**Fig. 1a**

153 and **1b**). Supplementation with both C and N (+C+N treatment) yielded an average net OD_{600} increase of

154 0.414 (**Fig. 1a**) and 0.506 (**Fig. 1c**) in the two sets of conducted experiments. Providing P_i in addition to C

155 and N (+C+N+P_i treatment) resulted in the largest growth (**Fig. 1a** and **Fig. 1c**). Interestingly, samples

156 that were supplemented with DNA instead of P_i (+C+N+H or +C+N+E treatments) also exhibited a

157 comparable amount of growth, although net OD_{600} increase was ~12.9% lower than in the +C+N+P_i

158 treatment (One-way ANOVA test; P-value 0.0036; **Fig. 1c**). Nevertheless, the net OD_{600} increases in the
159 +C+N+H and +C+N+E treatments were 50% and 54% higher, respectively, than in the +C+N treatment
160 (One-way ANOVA test; P-values 0.0023 and 0.0018, respectively; **Fig. 1c**). This suggests that besides P_i,
161 the saltern community can utilize eDNA as a source of phosphorus.

162 The observed patterns of microbial community growth under different treatments are consistent with
163 the consumed amounts of C, N, and P_i, as measured by comparing the total organic carbon (TOC), total
164 nitrogen (TN), and total phosphorus (TP) in the filtered untreated water samples and in the treated filtered
165 water samples after the communities reached the stationary phase. The pre-incubation communities
166 contained small quantities of TOC, TN, and TP (**Supplementary Table S1**). In treatments where
167 communities exhibited no notable growth (i.e., C was not provided), there were also no notable changes
168 in TOC, TP and TN (**Fig. 1d**). In the microcosms with some growth (C was provided but N was not), a
169 31-36% decrease in TN was observed (**Fig. 1d** and **Supplementary Table S1**), suggesting that growth
170 was sustained until naturally occurring utilizable nitrogen resources were depleted. The fastest growing
171 microcosms, i.e. in which both C and N were supplied, exhibited the largest decreases in TN, TP and TOC
172 (**Fig. 1d**).

173 To further investigate the effectiveness of DNA as a source of phosphorus, we examined the
174 contributions of inorganic (P_i) and organic (P_o) phosphorus to the TP in the microcosms after they reached
175 stationary phase (**Fig. 1e** and **Supplementary Table S2**). We found that in the microcosms supplemented
176 with C and N but not provided with P_i (i.e., +C+N, +C+N+H or +C+N+E treatments), the remaining TP
177 was dominated by P_o (~91%, ~70% and ~74%, respectively). Since the microcosms under the +C+N,

178 +C+N+H or +C+N+E treatments exhibited substantial growth, we conjecture that while DNA (i.e., P_o)

179 was used by the communities as a source of phosphorus, P_i is generally preferred when available.

180

181 **The taxonomic composition of the microbial communities and eDNA pool varies across treatments**

182 To better understand how the different nutrient availability affects both organismal composition of a

183 community and organismal sources of DNA in the eDNA pool, we sequenced 16S rRNA and *rpoB* genes

184 from the DNA extracted from the Isla Cristina living Cells (ICC) and the Isla Cristina Water column

185 (ICW) before and after the above-described microcosm experiments.

186 Analysis of the 16S rRNA OTUs revealed that, as expected for a saltern environment, the pre-

187 incubation community (ICC sample "X" on **Fig. 2a**) is numerically dominated by archaea from class

188 Halobacteria (relative abundance of 92.9%) and by bacteria from the genus *Salinibacter* (relative

189 abundance of 6.6%). The remaining 0.5% of OTUs belong to either other archaeal classes or other

190 bacterial genera (see **Supplementary Data**). Halobacteria and *Salinibacter* also dominate all post-

191 treatment communities, with their relative abundances in 92.3-99.9% and 0.02-7.2% range, respectively

192 (**Fig. 2a**).

193 The DNA in water column is also dominated by eDNA from Halobacteria and *Salinibacter* OTUs

194 (**Fig. 2a**). However, DNA originating from bacteria on average represents a higher fraction in the eDNA

195 pools than in the microbial communities, with the largest fraction (27%) found in the pre-incubation water

196 column (ICW sample "X" on **Fig. 2a)**. Additionally, some eDNA comes from OTUs that were either not

197 observed in any of the ICC samples (**Fig. 2b**) or were found in the ICC samples in low abundances.

198 Examples include OTUs from bacterial genus *Bradyrhizobium* and archaeal subphylum
199 Nanohaloarchaeota (see **Supplementary Results** and **Supplementary Data** for details). These eDNA
200 fragments may have originated from living microorganisms elsewhere and were transported to the saltern
201 environment. Alternatively, they may represent resistant-to-consumption eDNA that has slowly
202 accumulated from the rare members in the pre-incubation community (see **Supplementary Results** for
203 specific examples.)

204 Overall, OTUs present at >1% abundance constitute the greatest majority of OTUs in every sample
205 (**Fig. 2c**). Unfortunately, many haloarchaea are known to carry multiple non-identical copies of 16S rRNA
206 gene [37–39], with some copies exhibiting within-genome identity as low as 91.3% (**Supplementary**
207 **Table S5**). Since this intragenomic heterogeneity is likely to affect accuracy of the 16S rRNA-based
208 relative abundance estimates, we also amplified the *rpoB* gene, which is known to exist in haloarchaeal
209 genomes in a single copy, and was shown to resolve genera assignments better than the 16S rRNA gene
210 [40–42]. Because the 16S rRNA analysis indicates that the microbial communities are dominated by
211 Halobacteria and do not contain any OTUs from other archaeal classes at > 1% abundance, we amplified
212 the *rpoB* gene using the Halobacteria-specific primers. Of the 5 905 *rpoB*-based OTUs detected across all
213 samples, 5 851 (99.1%) are assigned to class Halobacteria, demonstrating that the primers designed to
214 amplify this class of Archaea have high specificity. Relative abundances of Halobacterial genera observed
215 in the *rpoB*-based and 16S rRNA-based analyses are comparable, with few discrepancies detailed in
216 **Supplementary Results**.

217 Thirty-four of the *rpoB*-based OTUs have > 1% relative abundance in at least one ICC sample.

218 Thirty two of the 34 OTUs maintain > 1% relative abundance in at least one ICW sample. Additional 29
219 halobacterial OTUs have > 1% relative abundance in at least one ICW sample, and found in low
220 abundance in at least one ICC sample. For the remainder of the analyses we designated these 34 + 29 = 63
221 OTUs as *abundant halobacterial OTUs* (ahOTUs). Notably, an individual sample contains only a fraction
222 of the 63 ahOTUs: 16 ± 1.8 of ahOTUs per ICC sample and 18 ± 2.8 ahOTUs per ICW sample. Because
223 in each sample the cumulative relative abundance of ahOTUs is 67-78% and 80 - 95% for ICC and ICW
224 samples, respectively (**Fig. 2d**), there are non-negligible differences in the ahOTU composition and their
225 relative abundances across samples. Below, we examine in detail how these differences relate to nutrient
226 availability.
227

228 **Carbon, DNA and inorganic phosphorus alter taxonomic composition of microbial communities**
229 **and eDNA pools**

230 Based on the relative abundances of both the *rpoB*-based and the 16S rRNA-based OTUs, the samples
231 aggregated into three distinct clusters **(Fig. 3** and **Supplementary Fig. S1a)**. Differences in OTU
232 composition of the three clusters are significant (PERMANOVA: R = 0.74, P = 0.001 [*rpoB*] and R =
233 0.72, P = 0.001 [16S rRNA]). Cluster 1 consists of the cellular communities' samples that come from the
234 pre-treatment and all microcosms that either exhibited no notable or some growth (**Fig. 1b**), hereafter
235 referred as "slow-growing communities". Cluster 2 consists of the water column samples that correspond
236 to the cellular communities of Cluster 1. Cluster 3 consists of the cellular communities' and water column
237 samples from all experiments that produced fast-growing microcosms, that is, the microcosms that were

238 supplemented simultaneously with C and N. Such clear taxonomic separation of fast- and slow-growing
239 microcosms suggests substantial shifts in community composition in response to nutrient
240 supplementation. Clusters 1, 2 and 3 also emerge even if OTU abundance is ignored and only OTU
241 richness is considered (**Supplementary Fig. S2**), suggesting that the observed clustering is not driven
242 solely by a few abundant community members, but also influenced by rare microorganisms and their
243 DNA in the water column.

244 Presence and abundance of specific bacterial and archaeal OTUs, and especially those with > 1%
245 abundance, are behind the observed shifts in taxonomic composition among the three clusters (**Fig. 2**).
246 Among Halobacteria, the relative abundances of 48 of the 63 ahOTUs differ significantly among the three
247 clusters (the Mann-Whitney *U* test; see **Supplementary Table S6** for P values; **Fig. 4a**). Cluster 1
248 samples are dominated mostly by Haloferacaceae ahOTUs (**Fig. 4b** and **4c**). In contrast, eDNA from
249 Halorubraceae ahOTUs (**Fig. 4b** and **4d**) dominate Cluster 2 samples. Finally, in Cluster 3 samples,
250 Haloferacaceae and Halorubraceae ahOTUs become much less abundant and are replaced by
251 Haloarculaceae and Halobacteriaceae ahOTUs (**Fig. 4b** and **4e**).

252 Within the three clusters, there are visibly distinct sub-clustering of samples that imply more
253 nuanced differences in taxonomic composition of the samples. For the Cluster 1 communities and their
254 water columns (Cluster 2), the pre-treatment sample, samples without notable growth (no C added) and
255 some growth (C added) form separate clusters, with further subdivision due to provision of *Hfx. volcanii*
256 DNA (PERMANOVA: R = 0.75 and 0.84, P = 0.001 and 0.001 [*rpoB*] and R = 0.74 and 0.81, P = 0.008
257 and 0.007 [16S rRNA]) (**Fig. 3b-c** and **Supplementary Fig. S1b-c**). Within fast-growing microcosms

258 (Cluster 3), sub-clustering is less pronounced but reflects availability and type of P sources provided in
259 treatments (**Fig. 3d** and **Supplementary Fig. S1d**). Taxonomically, the observed groups are due to
260 differences in relative abundance of Halorubraceae, Haloarculaceae and Haloferacaceae OTUs for slow-
261 growing communities and of Haloferacaceae, Halorubraceae, Haloarculaceae and Halobacteriaceae OTUs
262 in fast-growing communities (**Fig. 3e**).

263 Taken together, supplementation of nutrients significantly influences composition of both the
264 microbial community and the eDNA pool. Linear regression modeling with nutrients as categorical
265 variables revealed that provision of C is the primary driver of microbial community composition shifts
266 ($R_{adj}^2 = 0.45$; $P = 0.002$; *t* value: 4.5), suggesting unequal abilities of various taxa to compete for added
267 glucose. Provision of N alone does not affect community composition, suggesting that community
268 members have equal abilities in its assimilation. Provision of P_i and DNA significantly alters the
269 composition of eDNA in the water column ($R_{adj}^2 = 0.327$; $P = 0.001$; *t* value: 3.6), raising a possibility that
270 there are organismal preferences for phosphate and specific "taxonomic affiliation" of DNA as a P source.
271

272 **Shifts in eDNA OTU composition depending on available sources of phosphorus suggest**
273 **preferential eDNA uptake**

274 It is surprising that the DNA content of the initial community and the slow-growing microcosms (Cluster
275 1) are quite different from the eDNA pools of their water columns (Cluster 2). This distinction, albeit less
276 apparent, also exists in the fast-growing microcosms (Cluster 3; **Fig. 3d**). Assuming that all cells in a
277 microcosm have equal probability of birth and death, it would be expected to see similar OTU

278 compositions of a microbial community and of the eDNA from the corresponding water column.
279 Interestingly, in the slow-growing communities, provision of *Hfx. volcanii* DNA (+H and +C+H
280 treatments) significantly increases the eDNA OTU richness (the Mann-Whitney *U* test, $P = 1.6\times10^{-5}$;
281 **Supplementary Fig. S3**). In the fast-growing communities, the increase in eDNA OTU richness, albeit
282 not significant, is caused by the addition of P_i (+C+N+P_i treatment; **Supplementary Fig. S3**). Therefore,
283 we hypothesize that the observed differences in OTU compositions of cellular communities and their
284 water columns are due to biased eDNA uptake from certain taxonomic groups. Furthermore, we propose
285 that the availability of *Hfx. volcanii* DNA and inorganic phosphorus in slow- and fast-growing
286 communities, respectively, results in the reduced uptake of available eDNA as a P source, leading to
287 eDNA accumulation in the environment and causing the observed changes in eDNA OTU composition.
288 And in reverse, the observed limited OTU diversity when P sources are scarce may be due to depletion of
289 eDNA from specific taxa through taxonomically-biased eDNA uptake.
290

291 **Preferences for eDNA of specific taxonomic origins by the saltern microbial community**

292 Complexity and variability of microcosms across experimental treatments (**Fig. 3e**), as well as impacts of
293 sequencing depth and sequencing biases, make it difficult to establish exact eDNA preferences of specific
294 OTUs from our data. However, by comparing relative abundances of specific OTUs in microcosms with
295 and without additional P sources, we can indirectly infer some taxonomic biases of eDNA uptake in this
296 saltern microbial community as a whole. Specifically, we will continue to assume that all cells in a
297 microcosm have equal probability of birth and death. As a result, OTUs that do not substantially change

298 their relative abundance in treatments with and without an extra P source are not expected to show
299 substantial changes in the relative abundance of their eDNA in the water column. Deviations from these
300 patterns would suggest an eDNA uptake bias, and we developed and applied two metrics to quantify such
301 differences (see **Materials and Methods** for details).

302 From comparisons of slow-growing microcosms with and without added *Hfx. volcanii* DNA, we
303 found that when *Hfx. volcanii* DNA is not provided, eDNA from five Halorubraceae and Haloarculaceae
304 ahOTUs is depleted (see highlighted taxa in **Supplementary Fig. S4** and **Supplementary Table S7**) and
305 eDNA of 305 additional OTUs become undetectable in the water columns (**Supplementary Table S8**). Of
306 these 305 OTUs, 98 (32%) belong to Halorubraceae and Haloarculaceae families. These findings suggest
307 preferential consumption of Halorubraceae and Haloarculaceae eDNA in slow-growing microcosms. In
308 fast-growing microcosms, eDNA from Haloarculaceae, Halorubraceae and Halobacteriaceae ahOTUs are
309 depleted in water columns without provided P source (either *Hfx. volcanii* DNA, *E. coli* DNA or P_i; see
310 highlighted taxa in **Supplementary Fig. S5** and **Supplementary Table S9**). In comparisons between
311 +C+N and +C+N+P_i treatments, eDNA from 158 OTUs become depleted in the water column without P_i,
312 and 62 of the 158 OTUs (39%) belong to Haloarculaceae, Halorubraceae and Halobacteriaceae families
313 (**Supplementary Table S10**). These observations suggest preferential consumption of eDNA from these
314 three families in fast-growing microcosms. Interestingly, the most abundant of the depleted eDNA
315 belongs to ahOTUs from families that represent a substantial fraction of the microcosms (Halorubraceae
316 for the slow-growing and Haloarculaceae for the fast-growing communities; **Fig. 3e**), indicating that
317 eDNA most closely related to the most abundant OTUs in the community is preferentially consumed.

318 Intriguingly, several ahOTUs become depleted in the +C+N+P_i water columns when compared to the
319 other three treatments with fast growth (+C+N, +C+N+H, and +C+N+E) (**Supplementary Fig. S5** and
320 **Supplementary Table S9**), suggesting that some eDNA may be more preferred by some organisms than
321 inorganic phosphorus.

322 We also hypothesize that the saltern community can also utilize bacterial eDNA, which can be
323 exemplified by Chitinophagaceae DNA (**Supplementary Fig. S6**). Chitinophagaceae OTUs are not
324 detected in the pre-incubation cellular community sample, but their DNA is abundant in the pre-
325 incubation water column. Under all experimental treatments, the Chitinophagaceae OTUs continue to be
326 undetected in the microbial communities, suggesting they are at best extremely rare community members.
327 However, their DNA is either absent or found at very low abundance in the treatments' water columns,
328 suggesting that Chitinophagaceae eDNA in the initial, pre-incubation water column was consumed by the
329 microcosms' communities.

330 Provision of large amounts of *Hfx. volcanii* DNA allowed us to identify taxa that likely prefer to
331 utilize *Hfx. volcanii* DNA as a P source (**Supplementary Table S7**). For example, the ahOTU
332 *denovo3413*, which is assigned to *Haloarculaceae* family and has 91.4% of nucleotide identity to
333 *Halapricum* sp. strain SY-39 (MF443862.1), has the average relative abundance of 0.08% in the slow-
334 growing communities without provided *Hfx. volcanii* DNA and 0.05% in the corresponding water
335 columns. However, when *Hfx. volcanii* DNA is supplied, the abundance of *denovo3413* increases
336 significantly, to 4.6% in microbial communities and to 4.3% in the water column samples (the Mann-
337 Whitney *U* test, $P = 7.4\times10^{-5}$ and 1.1×10^{-5}, respectively).

338 The above inferences do rely on an assumption that all cells in a microcosm have equal probability
339 of birth and death, which may not hold. Future work that establishes relative growth rates of individual
340 OTUs in the community will allow more precise estimation of eDNA preferences.
341

342 **Provided nutrients can be predicted from taxonomic affiliations of microbial community members**
343 **and of water column DNA**

344 The shifts in community composition in response to availability of C, N, and P suggest that nutrients
345 provided in the experiments may be predictable from the OTU composition associated with DNA in cells
346 and dissolved in water columns. We designed a random forest classifier that takes ahOTU composition as
347 an input and predicts if a sample falls into one of the five treatment groups: "No C was provided (no C)",
348 "C but no N were provided (+C)", "Only C and N were provided (no P)", "C, N and P_i were provided
349 (+P_i)", or "C, N and DNA were provided (+H/+E)". We found that a random forest classifier achieves
350 95.5% accuracy in a 20-fold cross-validation and 94.6% accuracy in out-of-bag (OOB) error estimate.
351 These predictions have significantly higher accuracies than those obtained in the classifier trained on the
352 randomly shuffled samples (Student's *t* test, $P < 2.2*10^{-16}$ for cross validation approach [**Fig. 5a**] and
353 Kolmogorov-Smirnov test, $P < 2.2*10^{-16}$ for OOB approach [**Fig. 5b**]). Predictions remain robust even for
354 smaller training data sets (**Fig. 5c**). Overall, 63 ahOTUs can predict the available nutrients with the mean
355 prediction accuracy of 62%. The predictions are strongly influenced by 24 ahOTUs where each one
356 contributes ≥1% of the prediction accuracy (**Fig. 5d)** and their removal decreases the overall mean
357 classifier accuracy by 49%. Consistent with this observation, 23 of the 24 ahOTUs have significantly

358 different abundances in samples from the five groups (**Fig. 5e**; one-way ANOVA test, all 23 P values <

359 0.01).

360

361 **Discussion**

362 Our microcosm experiments with saltern-derived microbial communities revealed that carbon, nitrogen

363 and phosphorus are limiting nutrients of the microcosms, and by inference the Isla Cristina crystallizer

364 pond habitat, since their simultaneous provision resulted in the largest growth of cells. Having a readily

365 accessible carbon source is most crucial for this microbial community, because no notable growth was

366 observed without supplementation of carbon. Nitrogen, on the other hand, was more easily assimilated

367 from the naturally available sources, as microcosms with no supplemented nitrogen exhibited growth until

368 the environmental nitrogen was depleted. Interestingly, the communities supplied with carbon and

369 nitrogen grew well even if not supplied with inorganic phosphorus, suggesting that they were able to

370 utilize either provided DNA or naturally occurring eDNA as a source of phosphorus. However, eDNA

371 (while likely present in all experimental microcosms) evidently could not serve as a source of carbon and

372 nitrogen, for an unknown reason.

373 Nutrient usage of eDNA is not unique to the saltern microorganisms, as other microbes are known to

374 use DNA as a nutrient by enzymatic cleavage of eDNA (either extracellularly or intracellularly) into

375 deoxyribose, inorganic orthophosphate, and nucleobases [14, 17]. Yet, there is also a possibility that the

376 observed growth in our microcosms was instead due to utilization of internal cellular DNA as a source of

377 phosphorus. For example, previous experiments on a model haloarchaeon *Hfx. volcanii* demonstrated that

378 in the absence of supplemented phosphate *Hfx. volcanii* was able to utilize phosphate stored in dozens of

379 its chromosome and plasmids copies [23, 29]. Polyploidy was detected in all tested species and strains of
380 Haloarchaea, and may be common in Haloarchaea [43–45] and Euryarchaeota [46]. Hence, many
381 microorganisms populating the communities in our experiments could be polyploid and consequently
382 could use the extra copies of their chromosomes as a P source.

383 Given the presumed utilization of eDNA as a P source, it is puzzling why so much of the available
384 eDNA has remained unused. One possibility is that the community reached the stationary phase because it
385 ran out of other nutrients first. For instance, nitrogen was used up in the fast-growing communities
386 (**Supplementary Table S1**). Alternatively, the microorganisms may not have been able to utilize all
387 available eDNA. For instance, aquatic bacteria are hypothesized to specialize on different sizes of DNA
388 fragments [19], and naturally competent *Haemophilus influenzae* and *Neisseria gonorrhoeae* use species-
389 specific DNA uptake recognition sequences and therefore would not import each other's DNA [47–49].
390 DNA methylation patterns are also important for discriminating different sources of DNA during the
391 uptake process [23, 50]. As a result, some eDNA might not be recognized as a P source. Consistent with
392 these observations, the changes in eDNA composition of the water columns associated with our
393 experimental microcosms showed that organismal origin of eDNA indeed matters for growth on eDNA,
394 with some bacterial and archaeal eDNA being clearly preferred. Especially preferred is eDNA from the
395 most dominant members of the microcosms, suggesting some haloarchaea prefer eDNA that is most
396 closely related to their own. This preference may be based on DNA methylation patterns [23]. Future
397 studies are needed to better understand the specific reasons behind the observed biases in eDNA
398 utilization.

399 The observed patterns of preferential eDNA consumption and differential growth under various
400 nutrient availability regimes are associated with substantial shifts in the taxonomic composition and
401 overall diversity of underlying microcosm communities. While the "bottle effect" [51, 52] can never be
402 completely ruled out for any laboratory microcosm experiments, lack of growth and absence of rapid
403 changes in nutrient availability in the microcosms without provided nutrients, as well as similarity of the
404 pre-incubation and slow-growing communities, suggest that the observed substantial changes to
405 community composition occur in response to the addition of specific nutrient combinations rather than
406 due to the bottle effect. Therefore, we conjecture that in salterns the microbial community assembly is
407 determined by the available resources.
408 Such resource-based assembly also has been demonstrated in synthetic bacterioplankton
409 communities [53], and therefore may represent a general principle for a microbial community assembly.
410 The changes in a microbial community structure in response to environmental challenges are highly
411 dynamic [54], and are likely due to a combination of differential abilities of lineages to survive under
412 severe nutrient limitation [55, 56], to compete for assimilation of limited nutrients [57], to compete for
413 uptake of abundant nutrients [58], to inhibit growth of their competitors [59], and to create mutualistic
414 relationships via metabolic exchange and cross-feeding [54, 60]. Although relative importance of these
415 factors in our saltern community remains to be established, differential abundance of Haloferaceae,
416 Halorubraceae and Halobacteriaceae families in response to availability of carbon and phosphorus
417 indicate that competition for the available nutrients plays a major role in shaping saltern communities.
418 Moreover, after addition of limiting nutrients, the microcosms exhibited increased biomass production

419 and reduction in OTU richness. Such loss of species diversity in response to increase in nutrient
420 availability has been also demonstrated in bacterial biofilms [61], soil microbial communities [62],
421 phytoplankton [63] and plants [64], and was interpreted as a support for the niche dimensionality theory
422 [65]. The theory postulates that biodiversity is maintained under limiting resources because competition
423 for them can be achieved via different trade-offs, which in turn creates multiple niches that can be
424 occupied by similar but not identical species or lineages. Removing nutrient limitation eliminates trade-
425 offs and leads to a decreased diversity. Yet, presence of several closely related and abundant OTUs from
426 *Haloarcula* and *Halomicroarcula* genera in the fast-growing microcosms cannot be explained by
427 competition under the niche dimensionality framework. Therefore, other processes, such as mutual
428 exchange of metabolic by-products, may be at play to promote their coexistence [60]. Future
429 metagenomic surveys of metabolic genes within these microcosms will help to test this hypothesis.
430 Changing microbial communities can in turn have a great impact on the environment they inhabit
431 [66, 67] . By applying a machine learning algorithm to OTU abundance and nutrient treatments data from
432 our microcosm experiments, we found that the nutrient availability could be predicted with high accuracy
433 from the DNA composition of a microbial community and water column. Notably, to achieve the high
434 accuracy it is sufficient to have data from only few abundant OTUs. Our findings suggest that nutrient
435 availability in a natural environment (or its past and future changes) could be predicted from a taxonomic
436 survey of a microbial community, if appropriate training data from laboratory experiments is available.
437 This could become a useful tool for advancing our understanding of ecological processes happening in
438 particular environments and for practical applications, like bioremediation projects or treatments of

microbiome-impacted diseases.

Acknowledgements

We thank Drs. Antonio Ventosa, Paulina Corral, and Cristina Sánchez-Porro (University of Sevilla), who helped with saltern sampling. We also thank Dr. Jialiang Kuang (University of Oklahoma) for discussions about random forest predictions, and Dr. Shaopeng Li (East China Normal University) for discussions about community assembly and niche dimensionality. The work was supported through a NASA Exobiology award NNX15AM09G to R.T.P. and O.Z., and by the Simons Foundation Investigator in Mathematical Modeling of Living Systems award 327936 to O.Z.

Author contributions

Z.S.H., O.Z., and R.T.P. conceived the study. M.O. and A.M. performed the microcosm experiments, DNA extraction and sequencing. Z.S.H. performed the metagenomic and statistical analyses. Z.S.H., O.Z., R.T.P. and M.O. wrote the manuscript. All authors discussed the results and commented on the manuscript.

Competing interests

The authors declare no competing interests.

References

459 1. Karl DM, Bailiff MD. The measurement and distribution of dissolved nucleic acids in aquatic
460 environments. *Limnol Oceanogr* 1989; **34**: 543–558.
461 2. Paul JH, Cazares LH, David AW, DeFlaun MF, Jeffrey WH. The distribution of dissolved DNA in an
462 oligotrophic and a eutrophic river of Southwest Florida. *Hydrobiologia* 1991; **218**: 53–63.
463 3. Corinaldesi C, Beolchini F, Dell'anno A. Damage and degradation rates of extracellular DNA in marine
464 sediments: implications for the preservation of gene sequences. *Mol Ecol* 2008; **17**: 3939–3951.
465 4. Carini P, Marsden PJ, Leff JW, Morgan EE, Strickland MS, Fierer N. Relic DNA is abundant in soil and
466 obscures estimates of soil microbial diversity. *Nat Microbiol* 2016; **2**: 1–6.
467 5. Dell'Anno A, Danovaro R. Extracellular DNA plays a key role in deep-sea ecosystem functioning. *Science*
468 2005; **309**: 2179–2179.
469 6. Wilhelm SW, Suttle CA. Viruses and nutrient cycles in the sea: viruses play critical roles in the structure
470 and function of aquatic food webs. *BioScience* 1999; **49**: 781–788.
471 7. Fenchel T. The microbial loop – 25 years later. *J Exp Mar Biol Ecol* 2008; **366**: 99–103.
472 8. Azam F, Smith DC, Steward GF, Hagström Å. Bacteria-organic matter coupling and its significance for
473 oceanic carbon cycling. *Microb Ecol* 1994; **28**: 167–179.
474 9. Orellana MV, Pang WL, Durand PM, Whitehead K, Baliga NS. A role for programmed cell death in the
475 microbial loop. *PLoS One* 2013; **8**: e62595.
476 10. Steinmoen H, Knutsen E, Havarstein LS. Induction of natural competence in *Streptococcus pneumoniae*
477 triggers lysis and DNA release from a subfraction of the cell population. *Proc Natl Acad Sci USA* 2002;
478 **99**: 7681–7686.

479 11. Draghi JA, Turner PE. DNA secretion and gene-level selection in bacteria. *Microbiology* 2006; **152**: 2683–
480 2688.
481 12. Paul JH, Jeffrey WH, DeFlaun MF. Dynamics of extracellular DNA in the marine environment. *Appl*
482 *Environ Microbiol* 1987; **53**: 170–179.
483 13. Salter I. Seasonal variability in the persistence of dissolved environmental DNA (eDNA) in a marine
484 system: The role of microbial nutrient limitation. *PLoS One* 2018; **13**: e0192409.
485 14. Nielsen KM, Johnsen PJ, Bensasson D, Daffonchio D. Release and persistence of extracellular DNA in
486 the environment. *Environ Biosafety Res* 2007; **6**: 37–53.
487 15. Lorenz MG, Wackernagel W. Bacterial gene transfer by natural genetic transformation in the environment.
488 *Microbiol Mol Biol Rev* 1994; **58**: 563–602.
489 16. Tehei M, Franzetti B, Maurel M-C, Vergne J, Hountondji C, Zaccai G. The search for traces of life: the
490 protective effect of salt on biological macromolecules. *Extremophiles* 2002; **6**: 427–430.
491 17. Mulcahy H, Charron-Mazenod L, Lewenza S. *Pseudomonas aeruginosa* produces an extracellular
492 deoxyribonuclease that is required for utilization of DNA as a nutrient source. *Environ Microbiol* 2010;
493 **12**: 1621–1629.
494 18. Pinchuk GE, Ammons C, Culley DE, Li S-MW, McLean JS, Romine MF, et al. Utilization of DNA
495 as a sole source of phosphorus, carbon, and energy by *Shewanella* spp.: ecological and physiological
496 implications for dissimilatory metal reduction. *Appl Environ Microbiol* 2008; **74**: 1198–1208.
497 19. Lennon JT. Diversity and metabolism of marine Bacteria cultivated on dissolved DNA. *Appl Environ*
498 *Microbiol* 2007; **73**: 2799–2805.

499 20. Chen I, Dubnau D. DNA uptake during bacterial transformation. *Nat Rev Microbiol* 2004; **2**: 241–249.

500 21. Finkel SE, Kolter R. DNA as a nutrient: novel role for bacterial competence gene homologs. *J*
501 *Bacteriol* 2001; **183**: 6288–6293.

502 22. Vorkapic D, Pressler K, Schild S. Multifaceted roles of extracellular DNA in bacterial physiology. *Curr*
503 *Genet* 2016; **62**: 71–79.

504 23. Chimileski S, Dolas K, Naor A, Gophna U, Papke RT. Extracellular DNA metabolism in *Haloferax*
505 *volcanii*. *Front Microbiol* 2014; **5**.

506 24. Redfield RJ. Do bacteria have sex? *Nat Rev Genet* 2001; **2**: 634–639.

507 25. Palchevskiy V, Finkel SE. *Escherichia coli* competence gene homologs are essential for competitive
508 fitness and the use of DNA as a nutrient. *J Bacteriol* 2006; **188**: 3902–3910.

509 26. Oren A. Population dynamics of halobacteria in the Dead Sea water column1. *Limnol Oceanogr* 1983;
510 **28**: 1094–1103.

511 27. Elevi Bardavid R, Khristo P, Oren A. Interrelationships between *Dunaliella* and halophilic
512 prokaryotes in saltern crystallizer ponds. *Extremophiles* 2008; **12**: 5–14.

513 28. Ventosa A, de la Haba RR, Sánchez-Porro C, Papke RT. Microbial diversity of hypersaline
514 environments: a metagenomic approach. *Curr Opin Microbiol* 2015; **25**: 80–87.

515 29. Zerulla K, Chimileski S, Näther D, Gophna U, Papke RT, Soppa J. DNA as a phosphate storage
516 polymer and the alternative advantages of polyploidy for growth or survival. *PLoS One* 2014; **9**:
517 e94819.

518 30. Burnstein KL, Dyer DW, Sparling PF. Preferential uptake of restriction fragments from a gonococcal

519 cryptic plasmid by competent *Neisseria gonorrhoeae*. *Microbiology* 1988; **134**: 547–557.

520 31. Elkins C, Thomas CE, Seifert HS, Sparling PF. Species-specific uptake of DNA by gonococci is
521 mediated by a 10-base-pair sequence. *J Bacteriol* 1991; **173**: 3911–3913.

522 32. Smith HO, Gwinn ML, Salzberg SL. DNA uptake signal sequences in naturally transformable bacteria.
523 *Res Microbiol* 1999; **150**: 603–616.

524 33. Mell JC, Hall IM, Redfield RJ. Defining the DNA uptake specificity of naturally competent
525 Haemophilus influenzae cells. *Nucleic Acids Res* 2012; **40**: 8536–8549.

526 34. Caporaso JG, Kuczynski J, Stombaugh J, Bittinger K, Bushman FD, Costello EK, et al. QIIME allows
527 analysis of high-throughput community sequencing data. *Nat Methods* 2010; **7**: 335–336.

528 35. Cole JR, Wang Q, Cardenas E, Fish J, Chai B, Farris RJ, et al. The Ribosomal Database Project: improved
529 alignments and new tools for rRNA analysis. *Nucleic Acids Res* 2009; **37**: D141–D145.

530 36. Breiman L: Random forests. *Mach Learn* 2001; **45**: pp 5–32.

531 37. Mylvaganam S, Dennis PP. Sequence heterogeneity between the two genes encoding 16S rRNA from the
532 halophilic archaebacterium *Haloarcula marismortui*. *Genetics* 1992; **130**: 399–410.

533 38. Vreeland RH, Straight S, Krammes J, Dougherty K, Rosenzweig WD, Kamekura M. *Halosimplex*
534 *carlsbadense* gen. nov., sp. nov., a unique halophilic archaeon, with three 16S rRNA genes, that grows
535 only in defined medium with glycerol and acetate or pyruvate. *Extremophiles* 2002; **6**: 445–452.

536 39. Boucher Y, Douady CJ, Sharma AK, Kamekura M, Doolittle WF. Intragenomic heterogeneity and
537 intergenomic recombination among haloarchaeal rRNA Genes. *J Bacteriol* 2004; **186**: 3980–3990.

538 40. Case RJ, Boucher Y, Dahllöf I, Holmström C, Doolittle WF, Kjelleberg S. Use of 16S rRNA and *rpoB*

539 genes as molecular markers for microbial ecology studies. *Appl Environ Microbiol* 2007; **73**: 278–
540 288.
541 41. Ki J-S, Zhang W, Qian P-Y. Discovery of marine *Bacillus* species by 16S rRNA and *rpoB* comparisons
542 and their usefulness for species identification. *J Microbiol Methods* 2009; **77**: 48–57.
543 42. Vos M, Quince C, Pijl AS, Hollander M de, Kowalchuk GA. A Comparison of *rpoB* and 16S rRNA
544 as markers in pyrosequencing studies of bacterial diversity. *PLoS One* 2012; **7**: e30600.
545 43. Soppa J. Evolutionary advantages of polyploidy in halophilic archaea. *Biochem Soc Trans* 2013; **41**: 339–
546 343.
547 44. Breuert S, Allers T, Spohn G, Soppa J. Regulated polyploidy in halophilic Archaea. *PLoS One* 2006;
548 **1**: e92.
549 45. Ludt K, Soppa J. Polyploidy in halophilic archaea: regulation, evolutionary advantages, and gene
550 conversion. *Biochem Soc Trans* 2019; **47**: 933–944.
551 46. Soppa J. Ploidy and gene conversion in Archaea. *Biochem Soc Trans* 2011; **39**: 150–154.
552 47. Mathis LS, Scocca JJ. On the role of pili in transformation of *Neisseria gonorrhoeae*. *Microbiology,*
553 1984; **130**: 3165–3173.
554 48. Redfield RJ, Findlay WA, Bossé J, Kroll JS, Cameron AD, Nash JH. Evolution of competence and DNA
555 uptake specificity in the Pasteurellaceae. *BMC Evol Biol* 2006; **6**: 82.
556 49. Hamilton HL, Dillard JP. Natural transformation of *Neisseria gonorrhoeae*: from DNA donation to
557 homologous recombination. *Mol Microbiol* 2006; **59**: 376–385.
558 50. Beauchamp JM, Leveque RM, Dawid S, DiRita VJ. Methylation-dependent DNA discrimination in natural

559 transformation of *Campylobacter jejuni*. *Proc Natl Acad Sci USA* 2017; **114**: E8053–E8061.

560 51. Zobell CE, Anderson DQ. Observations on the multiplication of bacteria in different volumes of stored sea
561 water and the influence of oxygen tension and solid surfaces. *Biol Bull* 1936; **71**: 324–342.

562 52. Ionescu D, Bizic-Ionescu M, Khalili A, Malekmohammadi R, Morad MR, de Beer D, et al. A new tool for
563 long-term studies of POM-bacteria interactions: overcoming the century-old Bottle Effect. *Sci Rep* 2015;
564 **5**: 14706.

565 53. Fu H, Uchimiya M, Gore J, Moran MA. Ecological drivers of bacterial community assembly in synthetic
566 phycospheres. *Proc Natl Acad Sci USA* 2020; **117**: 3656–3662.

567 54. Zuñiga C, Li C-T, Yu G, Al-Bassam MM, Li T, Jiang L, et al. Environmental stimuli drive a transition from
568 cooperation to competition in synthetic phototrophic communities. *Nat Microbiol* 2019; **4**: 2184–2191.

569 55. Bergkessel M, Basta DW, Newman DK. The physiology of growth arrest: uniting molecular and
570 environmental microbiology. *Nat Rev Microbiol* 2016; **14**: 549–562.

571 56. Basta DW, Angeles-Albores D, Spero MA, Ciemniecki JA, Newman DK. Heat-shock proteases promote
572 survival of *Pseudomonas aeruginosa* during growth arrest. *Proc Natl Acad Sci USA* 2020; **117**: 4358–
573 4367.

574 57. Ni B, Colin R, Link H, Endres RG, Sourjik V. Growth-rate dependent resource investment in bacterial
575 motile behavior quantitatively follows potential benefit of chemotaxis. *Proc Natl Acad Sci USA* 2020;
576 **117**: 595–601.

577 58. Teeling H, Fuchs BM, Bennke CM, Krüger K, Chafee M, Kappelmann L, et al. Recurring patterns in
578 bacterioplankton dynamics during coastal spring algae blooms. *eLife* 2016; **5**: e11888.

579 59. Ratzke C, Gore J. Modifying and reacting to the environmental pH can drive bacterial interactions. *PLoS*
580 *Biol* 2018; **16**: e2004248.
581 60. Goldford JE, Lu N, Bajić D, Estrela S, Tikhonov M, Sanchez-Gorostiaga A, et al. Emergent simplicity in
582 microbial community assembly. *Science* 2018; **361**: 469–474.
583 61. Mitri S, Clarke E, Foster KR. Resource limitation drives spatial organization in microbial groups. *ISME J*
584 2016; **10**: 1471–1482.
585 62. Wang C, Liu D, Bai E. Decreasing soil microbial diversity is associated with decreasing microbial biomass
586 under nitrogen addition. *Soil Biol Biochem* 2018; **120**: 126–133.
587 63. Interlandi SJ, Kilham SS. Limiting resources and the regulation of diversity in phytoplankton
588 communities. *Ecology* 2001; **82**: 1270–1282.
589 64. Harpole WS, Sullivan LL, Lind EM, Firn J, Adler PB, Borer ET, et al. Addition of multiple limiting
590 resources reduces grassland diversity. *Nature* 2016; **537**: 93–96.
591 65. Hutchinson GE. Concluding Remarks. *Cold Spring Harb Symp Quant Biol.* Yale University, New
592 Haven, CT 1957, pp 415–427.
593 66. Baker BJ, Banfield JF. Microbial communities in acid mine drainage. *FEMS Microbiol Ecol* 2003; **44**:
594 139–152.
595 67. Turnbaugh PJ, Ley RE, Mahowald MA, Magrini V, Mardis ER, Gordon JI. An obesity-associated gut
596 microbiome with increased capacity for energy harvest. *Nature* 2006; **444**: 1027–1031.
597
598

599 **Figure Legends**

600

601 **Figure 1. Microbial growth and associated changes in available nutrients in the experimental**

602 **microcosms. (a-c)** Growth curves under experimental treatments. Each line represents a separate

603 experimental treatment. For each treatment, the added nutrients are denoted as "+" followed by a nutrient

604 symbol of carbon (C), nitrogen (N), phosphorus (P_i), *Hfx. volcanii* DS2 DNA (H) and *E. coli dam*$^-$*/dcm*$^-$

605 DNA (E). Starvation growth curve (S) serves as a control. Error bars represent the standard error of the

606 mean. **Panel b** shows growth curves of the slow-growing microcosms from **panel a** plotted on a different

607 scale. **Panels a** and **c** represent two independent sets of experiments. **(d, e)** Change in carbon, nitrogen

608 and phosphorus after the microbial growth has stopped**.** The plotted changes are mean values from two

609 experimental replicates. The experimental treatments (X axis) are grouped into three categories based on

610 whether carbon and/or nitrogen were provided. Nutrient abbreviations: TOC, total organic carbon; TN,

611 total nitrogen; TP, total phosphorus; P_i, inorganic phosphorus. Organic phosphorus (P_o) was computed as

612 by subtracting P_i from TP. For "+P_i" treatment, the calculated value of P_o is replaced with an asterisk, due

613 to errors associated with measurements of TP and P_i for that treatment. Actual values for the measured

614 nutrient concentrations and the associated calculations are shown in **Supplementary Tables S1** and **S2**.

615

616 **Figure 2. OTU composition of the microbial communities (ICC) and of eDNA in the associated**

617 **water columns (ICW). (a)** Relative abundance of 16S rRNA-based OTUs in the pre-incubation

618 community (X), after starvation (S), and after nutrient-addition experiments. For experimental treatment

619 abbreviations see **Figure 1** legend. Only a few selected taxonomic groups are highlighted, while other
620 OTUs are pooled into "Other Archaea" and "Other Bacteria" categories. **(b)** Overlap of 16S rRNA-based
621 OTUs in ICC and ICW across all samples combined. **(c)** Relative abundances of 16S rRNA-based OTUs
622 that constitute ≥ 1% of at least one sample (designated as "abundant OTUs") in comparison to the OTUs
623 with < 1% abundance (denoted as "Other OTUs"). **(d)** Relative abundances of *rpoB*-based OTUs from
624 class Halobacteria that constitute ≥ 1% of at least one sample (designated as "ahOTUs") in comparison to
625 the Halobacterial OTUs with < 1% abundance (denoted as "Other Halobacterial OTUs").
626
627 **Figure 3. Comparison of the *rpoB*-based OTU compositions of the analyzed samples.** (**a**) Principal
628 Coordinate Analysis (PCoA) of all samples using the pairwise Bray-Curtis dissimilarity as a distance
629 metric. The distances were calculated using all OTUs in a sample. Circles denote microbial community
630 samples, while triangles refer to the water column samples. Within these, samples for treatments with
631 added DNA are shown using filled symbols, while all remaining samples are shown using open symbols.
632 For the PCoA analyses carried out using 16S rRNA-based OTUs, see **Supplementary Figure S2**. (**b**, **c**
633 and **d**) PCoA of the samples within each of the three clusters. Same distance measure and same symbol
634 notations as in panel **a**. (**e**) Taxonomic composition of samples within each of the three clusters. See
635 **Supplementary Table S4** for the actual relative abundance values.
636
637 **Figure 4. Relative abundance of ahOTUs across three clusters.** (**a** and **b**) Relative abundance of
638 ahOTUs in three clusters summarized in a ternary plot. Each vertex represents one of the three clusters.

639 Each circle represents an ahOTU. The position of a circle is determined by relative abundance (RA) of the
640 ahOTU in three clusters, and the circle size is proportional to the ahOTU's average relative abundance
641 across all 69 samples. In **panel a**, ahOTUs with significantly higher abundance in Cluster 1, 2 or 3 than in
642 the other two clusters are colored in green, orange and brown, respectively, while OTUs without
643 significant difference in abundance are shown in grey. In **panel b**, the circles are colored according to the
644 taxonomic assignment of the ahOTUs. (**c, d** and **e**) Aggregated relative abundances (aRA) of ahOTUs
645 with significantly higher abundance in one cluster across each of the three clusters. Each point represents
646 an ahOTU. For each OTU its aRA in a cluster *i* (*i = 1,2,3*) is defined as $aRA_i = \frac{RA_i}{\sum_{j=1}^{3}(RA_j)}$, where RA_i is
647 the relative abundance of the ahOTU in the cluster *i*. The distribution of aRAs within a cluster is
648 summarized by a probability density function and a box-and-whisker plot, with whiskers extending to 1.5
649 of the interquartile range.
650
651 **Figure 5. Performance of a random forest classifier in predicting available nutrients from the OTU**
652 **composition of a microbial community.** (**a**) Prediction accuracy in the 20-fold cross-validation of the
653 classifier across 1000 training/validation datasets constructed from real and randomly reshuffled data. (**b**)
654 Distribution of the out-of-bag (OOB) errors across 1000 training/validation datasets constructed from real
655 and randomly reshuffled data. (**c**) Changes in prediction accuracy with the dataset size, which is shown as
656 percent of the 69 samples used and as the leave-one-out strategy. (**d**) The decrease in prediction accuracy
657 of 24 ahOTUs with at least 1% contribution to the predicted accuracy. The OTUs are colored according to
658 notations shown in **Figure 3**. (**e**) The relative abundance of the top 24 ahOTUs in five categories of

659 treatments. For each OTU, the relative abundance values were transformed into heatmap colors. The

660 OTUs are clustered based on their relative abundance across five categories (as described in **Methods**).

661 Abbreviations of five treatment categories: "+C", C but no N were provided; "no C", No C was provided;

662 "+H/+E", C, N and DNA was provided; "+P_i", C, N and P_i were provided; "No P", only C and N were

663 provided.

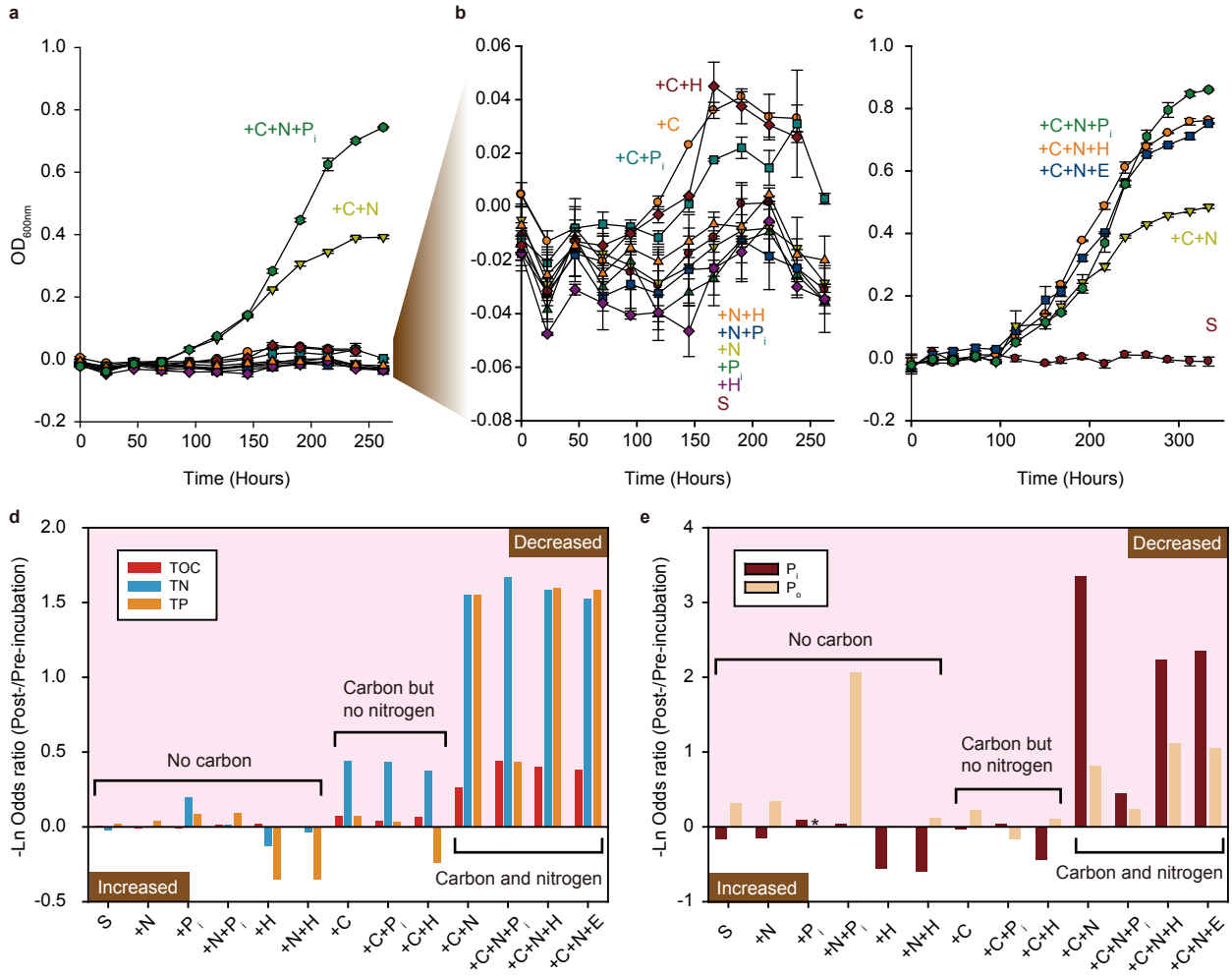
a
b
c
d
e
OD600nm
Time (Hours)
+C+N+Pi
+C+N
+C+H
+C
+C+Pi
+N+H
+N+Pi
+N
+Pi
+H
S
+C+N+H
+C+N+E
TOC
TN
TP
Decreased
Increased
No carbon
Carbon but no nitrogen
Carbon and nitrogen
-Ln Odds ratio (Post-/Pre-incubation)
Pi
Po
S
+N
+Pi
+N+Pi
+H
+N+H
+C
+C+Pi
+C+H
+C+N
+C+N+Pi
+C+N+H
+C+N+E

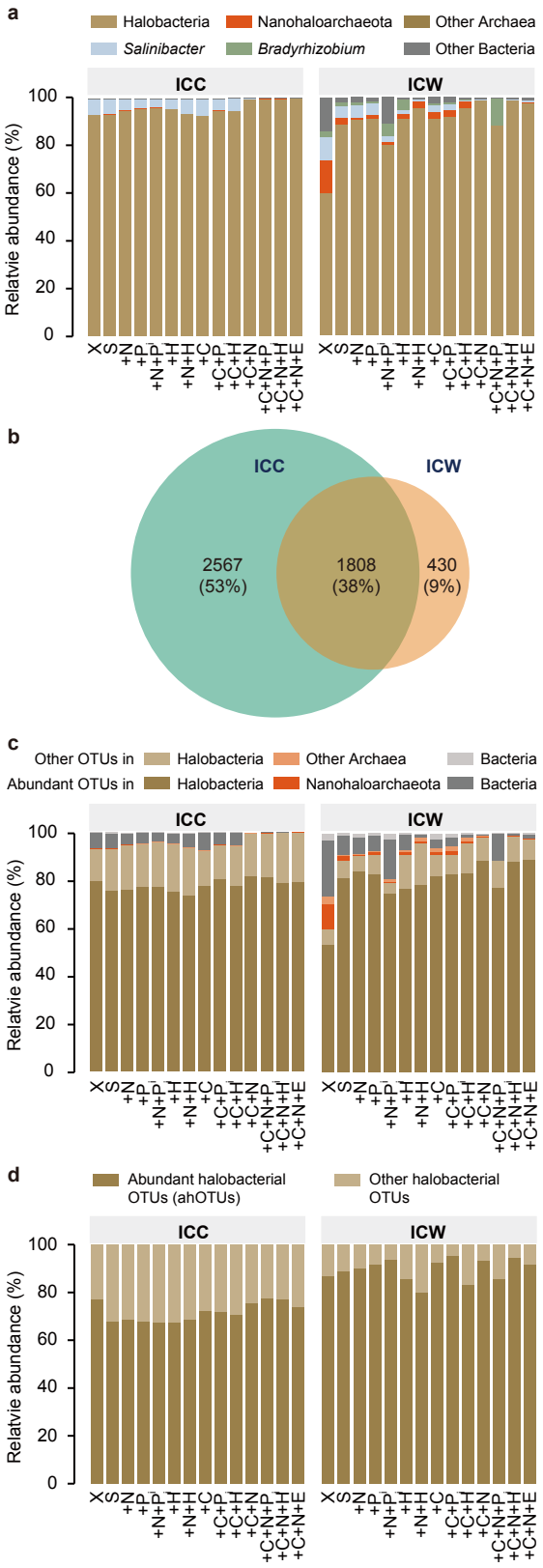
a
Halobacteria
Nanohaloarchaeota
Other Archaea
Salinibacter
Bradyrhizobium
Other Bacteria
ICC
ICW
Relatvie abundance (%)
100
80
60
40
20
0
b
ICC
ICW
2567
(53%)
1808
(38%)
430
(9%)
c
Other OTUs in
Halobacteria
Other Archaea
Bacteria
Abundant OTUs in
Halobacteria
Nanohaloarchaeota
Bacteria
ICC
ICW
Relatvie abundance (%)
d
Abundant halobacterial OTUs (ahOTUs)
Other halobacterial OTUs
ICC
ICW
Relatvie abundance (%)

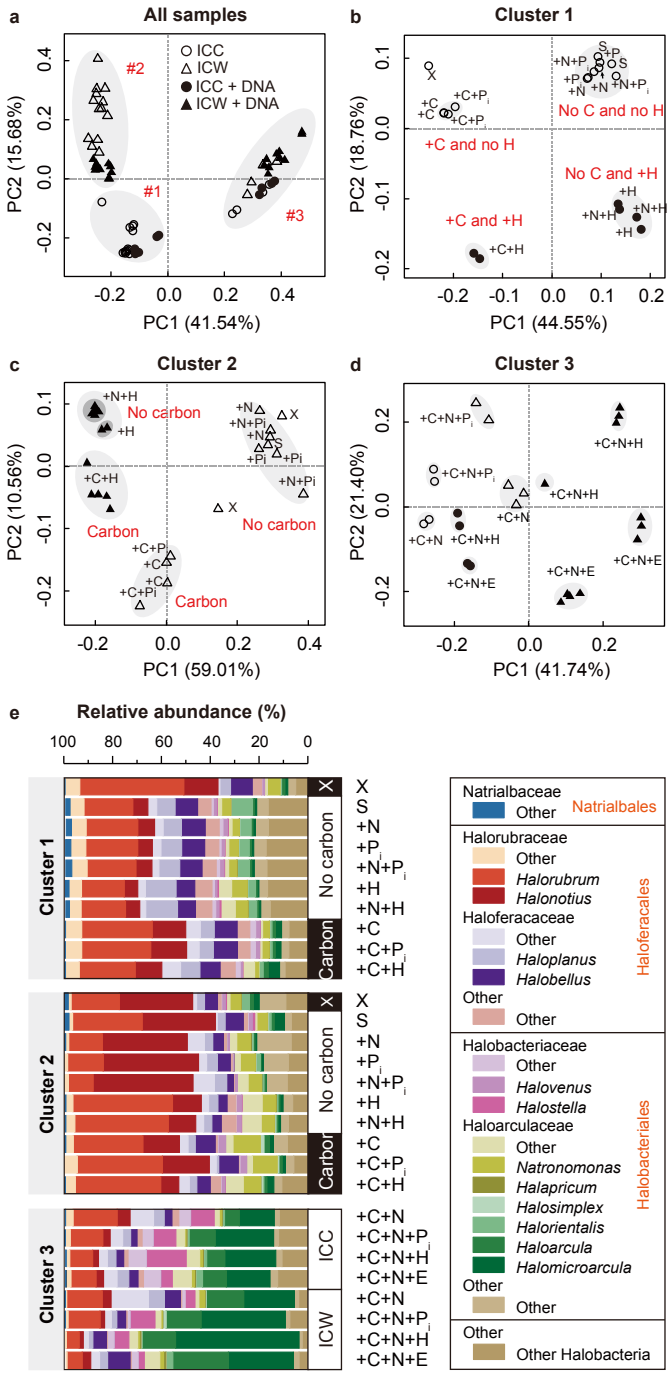
a
All samples
ICC
ICW
ICC + DNA
ICW + DNA
#1
#2
#3
PC1 (41.54%)
PC2 (15.68%)
b
Cluster 1
No C and no H
+C and no H
No C and +H
+C and +H
PC1 (44.55%)
PC2 (18.76%)
c
Cluster 2
No carbon
Carbon
PC1 (59.01%)
PC2 (10.56%)
d
Cluster 3
PC1 (41.74%)
PC2 (21.40%)
e
Relative abundance (%)
Cluster 1
Cluster 2
Cluster 3
No carbon
Carbon
ICC
ICW
X
S
+N
+Pi
+N+Pi
+H
+N+H
+C
+C+Pi
+C+H
+C+N
+C+N+Pi
+C+N+H
+C+N+E
Natrialbaceae
Other
Natrialbales
Halorubraceae
Other
Halorubrum
Halonotius
Haloferacaceae
Other
Haloplanus
Halobellus
Haloferacales
Halobacteriaceae
Halovenus
Halostella
Haloarculaceae
Natronomonas
Halapricum
Halosimplex
Halorientalis
Haloarcula
Halomicroarcula
Halobacteriales
Other Halobacteria

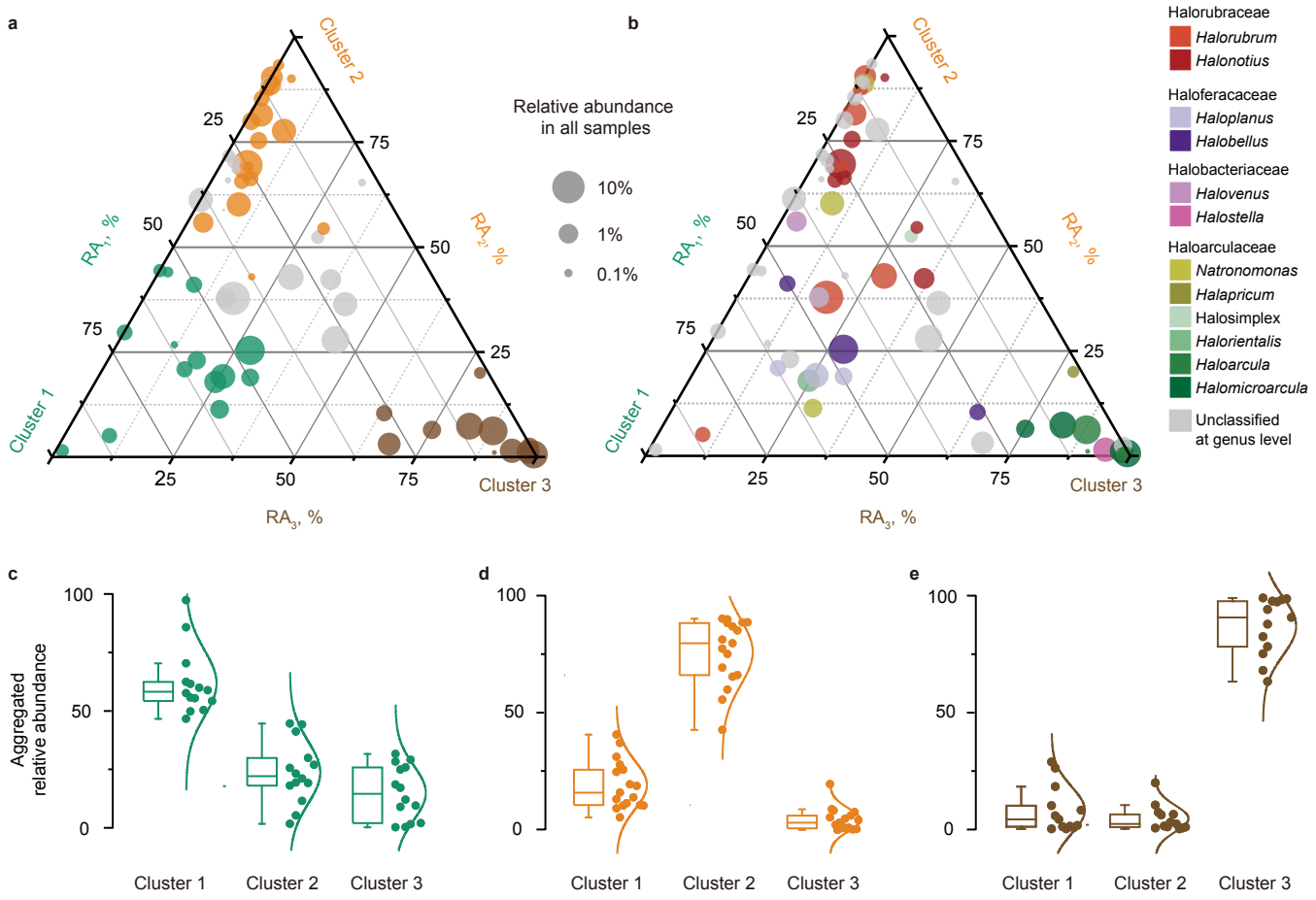
a
b
Cluster 1
Cluster 2
Cluster 3
RA1, %
RA2, %
RA3, %
25
50
75
Relative abundance
in all samples
10%
1%
0.1%
Halorubraceae
Halorubrum
Halonotius
Haloferacaceae
Haloplanus
Halobellus
Halobacteriaceae
Halovenus
Halostella
Haloarculaceae
Natronomonas
Halapricum
Halosimplex
Halorientalis
Haloarcula
Halomicroarcula
Unclassified
at genus level
c
d
e
Aggregated
relative abundance
100
50
0
Cluster 1
Cluster 2
Cluster 3

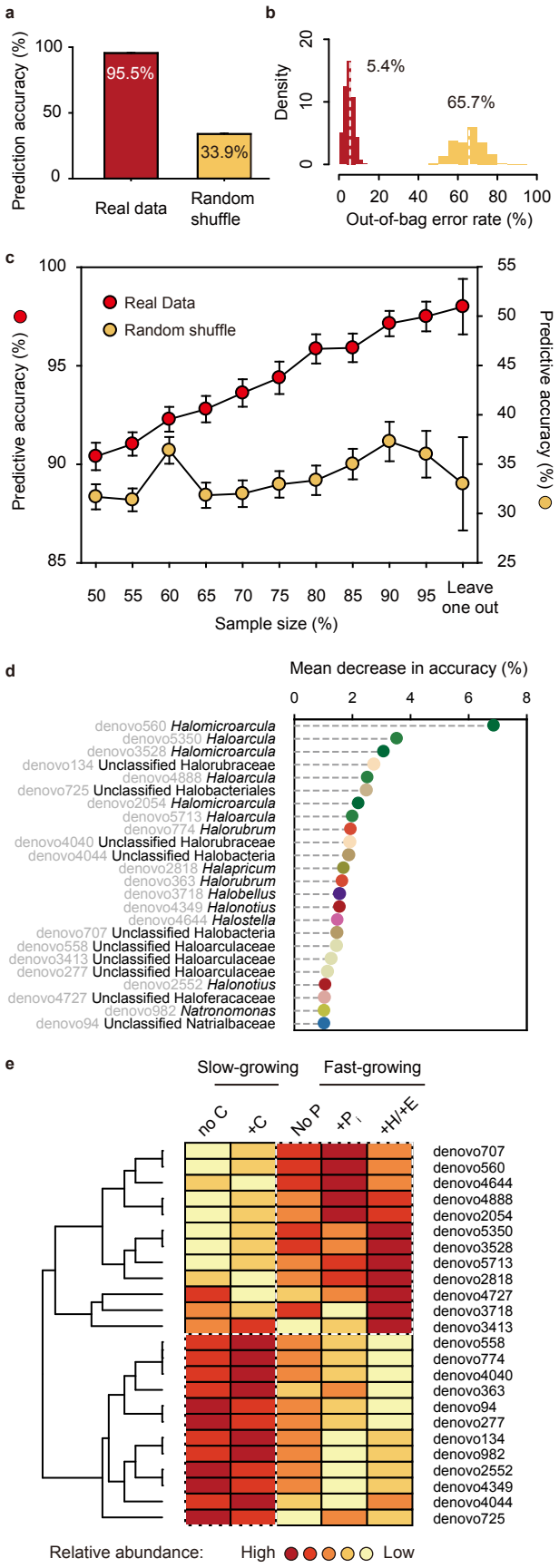
a
Prediction accuracy (%)
100
50
0
95.5%
33.9%
Real data
Random shuffle
b
Density
20
10
0
5.4%
65.7%
0 20 40 60 80 100
Out-of-bag error rate (%)
c
Real Data
Random shuffle
Predictive accuracy (%)
100
95
90
85
55
50
45
40
35
30
25
50 55 60 65 70 75 80 85 90 95 Leave one out
Sample size (%)
d
Mean decrease in accuracy (%)
0 2 4 6 8
denovo560 Halomicroarcula
denovo5350 Haloarcula
denovo3528 Halomicroarcula
denovo134 Unclassified Halorubraceae
denovo4888 Haloarcula
denovo725 Unclassified Halobacteriales
denovo2054 Halomicroarcula
denovo5713 Haloarcula
denovo774 Halorubrum
denovo4040 Unclassified Halorubraceae
denovo4044 Unclassified Halobacteria
denovo2818 Halapricum
denovo363 Halorubrum
denovo3718 Halobellus
denovo4349 Halonotius
denovo4644 Halostella
denovo707 Unclassified Halobacteria
denovo558 Unclassified Haloarculaceae
denovo3413 Unclassified Haloarculaceae
denovo277 Unclassified Haloarculaceae
denovo2552 Halonotius
denovo4727 Unclassified Haloferacaceae
denovo982 Natronomonas
denovo94 Unclassified Natrialbaceae
e
Slow-growing
Fast-growing
no C
+C
No P
+Pi
+H/+E
denovo707
denovo560
denovo4644
denovo4888
denovo2054
denovo5350
denovo3528
denovo5713
denovo2818
denovo4727
denovo3718
denovo3413
denovo558
denovo774
denovo4040
denovo363
denovo94
denovo277
denovo134
denovo982
denovo2552
denovo4349
denovo4044
denovo725
Relative abundance:
High
Low